Polyester Biocomposites from Recycled Natural Fibers: Characterization and Biodegradability

Shuenn-Kung Su, Chin-San Wu

Department of Polymer Engineering, National Taiwan University of Science and Technology, Taipei, Taiwan 106, Republic of China

Received 14 October 2009; accepted 13 May 2010
DOI 10.1002/app.32808
Published online 2 August 2010 in Wiley Online Library (wileyonlinelibrary.com).

ABSTRACT: The structure, biodegradability, and morphological properties of composite materials composed of poly(butylene succinate adipate) (PBSA) and bamboo fiber (BF) were evaluated. Composites containing acrylic acid-grafted PBSA (PBSA-*g*-AA/BF) exhibited noticeably enhanced compatibility between the two components. The dispersion of BF in the PBSA-*g*-AA matrix was highly homogeneous as a result of ester formation and the consequent creation of branched and crosslinked macromolecules between the carboxyl groups of PBSA-*g*-AA and hydroxyl groups in BF. In addition, the PBSA-*g*-AA/BF composite was more easily processed due to a lower melt viscosity. Each composite was subjected to biodegradation tests in an *Acinetobacter baumannii* compost. Morphological observations indicated severe disruption of film structure after 10–20 days of incubation, and both the PBSA and the PBSA-*g*-AA/BF composite films were eventually completely degraded. The PBSA-*g*-AA/BF films were more biodegradable than those made of PBSA and exhibited a lower molecular weight and intrinsic viscosity, implying a strong connection between these characteristics and biodegradability. © 2010 Wiley Periodicals, Inc. J Appl Polym Sci 119: 1211–1219, 2011

Key words: biodegradation; bamboo fiber; polyesters; biocomposites

INTRODUCTION

Recently, the nonbiodegradability of plastics has caused extensive environmental problems associated with their disposal. Although recycling is an environmentally attractive solution, only a small percentage of plastics are actually recyclable, and most end up in municipal landfills. This perpetuates the increasingly difficult problem of finding available landfill sites. As a result, interest has grown in the production and use of materials that are renewable, degradable, and recyclable, better known as "green materials."[1–5] Bamboo fiber (BF) is an abundant natural fiber resource that requires only several months to grow to maturation in Asia and South America. The structure of bamboo is derived from fibers running longitudinally along its length, and it has been used historically to construct various living tools and facilities.[6] To practically apply the benefits of BFs to composite materials, one must extract the fibers in a qualitatively controlled manner.

Because BFs are covered with lignin, they are often brittle and are best applied as reinforcement in synthetic composite materials. Studies of BF-reinforced plastic composites have resulted in several publications,[7–10] but because the hydrophilic fibers do not adhere well to the hydrophobic polymer matrix, composites of plastics and natural fibers in many cases have poor mechanical properties. To solve this problem, reactive functional groups can be incorporated into the synthetic polymer to serve as compatibilizers to enhance the miscibility and improve the mechanical properties of the composites.[11,12] Maleated polypropylene copolymer is an effective compatibilizer in polypropylene/bamboo fiber (PP/BF) composites,[13] and coupling agents have been used to increase the compatibility between polymer and bamboo fibers.[14]

Many biocomposites of biodegradable polymers and natural fibers have demonstrated complete degradation in soil or compost without the emission of any toxic or noxious components and have, therefore, received a great deal of attention in composite science.[15] Several biodegradable aliphatic polymers such as poly(butylene succinate adipate) (PBSA), poly(3-hydroxybutyrate) (PHB), poly(butylene succinate) (PBS), and poly(lactic acid) (PLA) are of increasing commercial interest. As opposed to conventional plastics such as polystyrene (PS) and polyethylene (PE), which require hundreds or even thousands of years to degrade, PBSA can degrade into naturally occurring products in just a few years.[16] PBSA is also noted for its flexibility and can be produced by polymerization of glycols with dicarboxylic acids.[17,18] PBSA has been used in composites with other polymers as a packaging material and has been proposed for use in biomedical applications, including catheters, blood bags, and packaging.[19] As with other

Correspondence to: C.-S. Wu (cws1222@cc.kyu.edu.tw).

aliphatic polyesters,[20] the biocompatibility of PBSA and its copolymers has led to several commercially successful applications. Unfortunately, PBSA is relatively expensive. One way to reduce the cost of PBSA composites is by blending them with natural biomaterials. Dried BF has been widely applied in thermoplastic composites, but BFs ranging in length from millimeters to a centimeter do not mix well in polyester matrices and require a compatibilizing agent to wet the fibers.[6] In contrast, the higher hydrophilicity of PBSA-*g*-AA results in a natural wetting of BF. Composites of PBSA and BF, therefore, offer advantages in both biocompatibility and cost.[21]

Bamboo is an abundant natural fiber resource with high strength. When the PBSA-*g*-AA composites with BF, the composite would improve several properties (mechanical, biodegradable, and morphological properties) to be a useful material with lower cost. Even better, both PBSA and BF were biodegradable and absolutely harmless on environment, better known as "green materials." This report characterizes the physical properties and biodegradability of BF composites with PBSA and acrylic acid (AA)-grafted PBSA (PBSA-*g*-AA). The composites were characterized using Fourier transform infrared spectroscopy (FTIR) and ^{13}C nuclear magnetic resonance (NMR) to identify bulk structural changes induced by the acrylic acid moiety. In addition, the effects of BF content on water absorption and biodegradability were assessed for both the PBSA/BF and PBSA-*g*-AA/BF composites.

EXPERIMENTAL

Microbiological sample preparation

Acinetobacter baumannii (BCRC 15556) was supplied by the Bioresource Collection and Research Center in Taiwan. The strain was cultivated at 37°C and stirred at 200 rpm in nutrient broth (NB) (Difco) consisting of 3 g beef extract, 5 g peptone, and 1.0 L distilled water at pH 7.0. The culture was collected in its early stationary phase for cell entrapment.

Materials

Poly(butylene succinate adipate) was supplied by Mitsubishi Chemical Co. (Tokyo, Japan) and had an average molecular weight (M_w) of 1.53×10^5, a polydispersity index of 1.86, and an intrinsic viscosity (η) of 2.63 dL/g. Acrylic acid (AA), obtained from Sigma (St. Louis, MO), was purified before use by recrystallization from chloroform. Benzoyl peroxide (BPO; Sigma) was used as an initiator and was purified by dissolution in chloroform and reprecipitation in methanol. BF was obtained from Pingtung. PBSA-*g*-AA was synthesized according to previously published procedures[22] and had a M_w of 1.26×10^5, a polydispersity index of 2.32, and an η of 2.48 dL/g. The grafting percentage of PBSA-*g*-AA was $\sim$ 6.96 wt %. At such a low degree of grafting, the PBSA-*g*-AA structure was not noticeably different from that of PBSA. A slight decrease in M_w and intrinsic viscosity was apparent in the PBSA-*g*-AA compared with PBSA and was attributed to bond cracking induced by the grafting reaction.

PBSA-*g*-AA copolymer

Acrylic acid was grafted onto molten PBSA in a tetrahydrofuran solution under a nitrogen atmosphere at 50°C $\pm$ 2°C, and the polymerization reaction was initiated with BPO. The reaction system was stirred at 60 rpm for 6 h. The grafted product (4 g) was then dissolved in 200 mL refluxing tetrahydrofuran at 50°C $\pm$ 2°C, and the hot solution was filtered through several layers of cheesecloth. The cheesecloth was washed with acetone to remove the tetrahydrofuran-insoluble unreacted acrylic acid, and the product was dried on the cheesecloth in a vacuum oven at 80°C for 24 h. The tetrahydrofuran-soluble products in the filtrate were extracted five times using 600 mL cold acetone in each extraction. The subsequent grafting percentage was about 6.96 wt % by titration.[22] BPO and AA loading were maintained at 0.3 wt % and 10 wt %, respectively.

Bamboo fiber processing

As by-products of bamboo processing, bamboo fiber (BF) was extracted from 3- to 5-year old moso bamboo (*Phyllostachys pubescens* Mazel) from Chu-Shan in Taiwan. Bamboo, which contains a drinkable juice within the green outer shell, also contains a white fibrous material $\sim$ 1–2 cm thick. A sample of this material (600 g) was blended and dried in a reactor under vacuum (less than 10 mbar) at 90°C for 1 h. Sodium methoxide (0.3%) was added to the reactor, and the reaction was quenched after $\sim$ 1 day by adding water at 70–80°C. The product was washed five times and dried for 50 min under vacuum. After drying, the middle core contained light yellow fibers up to 5–8 cm long. The green outer shell was dried and ground, and the resulting fibers were sorted. BF samples obtained before grinding consisted of a mixture of fine brown powder with dispersed pale yellow single fibers up to 100–500 μm long. The samples were passed through 60-mesh (0.246 mm) and 80-mesh (0.175 mm) sieves, air-dried for 24 h at 70–80°C, and vacuum dried for at least 2 h at 115°C until the moisture content fell to 5% $\pm$ 1%.

Composite preparation

Before composite fabrication, BF samples were cleaned with acetone and dried in an oven at 105°C

for 24 h. Composites were prepared in a "Plastograph" 200-Nm Mixer W50EHT with a blade rotor (Brabender, Dayton, OH). The blends were mixed between 100°C and 110°C for 15 min at a rotor speed of 50 rpm. Samples were prepared with mass ratios of BF to PBSA or to PBSA-*g*-AA of 5/95, 10/90, 15/85, and 20/80. Residual AA in the PBSA-*g*-AA reaction mixture was removed via acetone extraction before the preparation of PBSA-*g*-AA/BF. After mixing, the composites were pressed into thin plates with a hot press and placed in a dryer for cooling. These thin plates were cut to standard sample dimensions for further characterization.

NMR/FTIR/GPC analyses

Solid-state ^{13}C-NMR spectra were obtained on a Bruker AMX 400 NMR spectrometer (Bruker BioSpin, Germany) at 100 MHz under cross-polarization while spinning at the magic angle. Power decoupling conditions were set with a 90° pulse and a 4-s cycle time. Infrared spectra of the samples were obtained using a Bio-Rad FTS-7PC FTIR spectrophotometer. Gel permeation chromatography (GPC) was performed using a Perkin-Elmer Series 200 system (Shelton, CT) at 40°C. In conducting GPC analyses, chloroform was used as an effluent at a flow rate of 1.0 mL/min using a Jordi Gel DVB 10000A gel column and a RI 71 detector. Polystyrene was used as a standard.

Composite morphology

A thin film of each blend was created with a hydrolytic press and treated with hot water at 80°C for 24 h before being coated with gold. The surface morphology of these thin films was observed using a scanning electron microscope (SEM, Hitachi Microscopy Model S-1400, Tokyo, Japan).

Water absorption

Samples were prepared for water absorption measurements by cutting them into 60 mm × 25-mm strips (150 ± 5 μm thickness) following the standard method of ASTM D570-81. The samples were dried in a vacuum oven at 50°C ± 2°C for 8 h, cooled in a desiccator, and then immediately weighed to the nearest 0.001 g (this weight was designated W_c). Thereafter, the samples were immersed in distilled water and maintained at 25°C ± 2°C for a 6-week period. During this time, they were removed from the water at 5-day intervals, gently blotted with tissue paper to remove excess water from their surfaces, immediately weighed to the nearest 0.001 g (this weight was designated W_w), and returned to the water. Each W_w is an average value obtained from three measurements. The percentage of weight increase due to water absorption (W_f) was calculated to the nearest 0.01% according to eq. (1):

$$\%W_f = \frac{W_w - W_c}{W_c} \times 100\%. \quad (1)$$

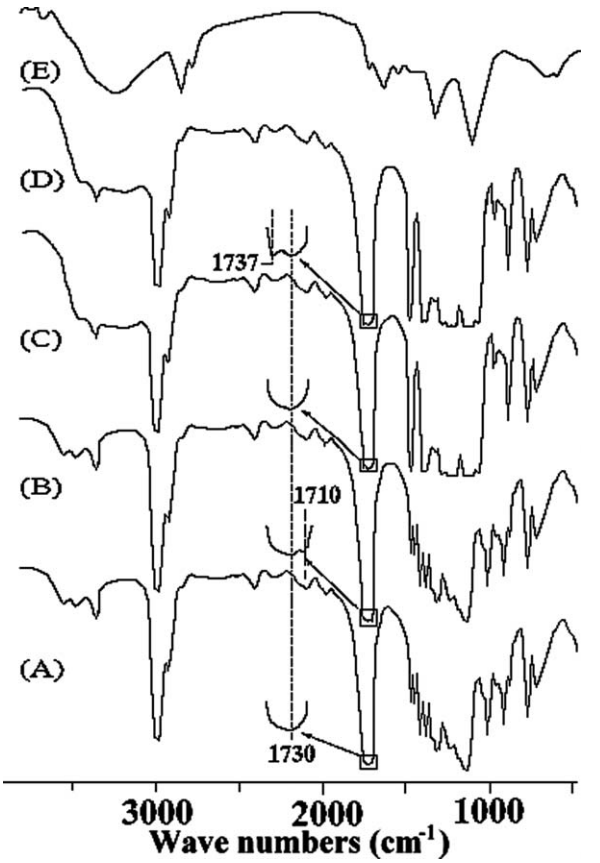

Figure 1 FTIR spectra are given for (A) PBSA, (B) PBSA-*g*-AA, (C) PBSA/BF (10 wt %), (D) PBSA-*g*-AA/BF (10 wt %), and (E) BF.

Biodegradation test

The biodegradability of the samples was assessed by evaluating the weight loss of composites over time in nutrient broth environment. Samples were cast into films using a 50 mm × 50 mm plastic mold. Films were removed from the mold and rinsed several times with distilled water until the waste water had a neutral pH. The films were then clamped to a glass sheet and dried in a vacuum oven (50°C ± 2°C, 0.5 mmHg, 24 h). After drying, the films were 0.05 mm ± 0.02 mm thick.

The dried films were placed in compost Petri dishes containing 30 mL of NB broth with *A. baumannii* and incubated at pH 7.0 ± 0.5, 35°C ± 2°C, and 50% ± 5% relative humidity. After incubation, the films were washed extensively with deionized water and dried. Each study was conducted using three replicate compost dishes and three

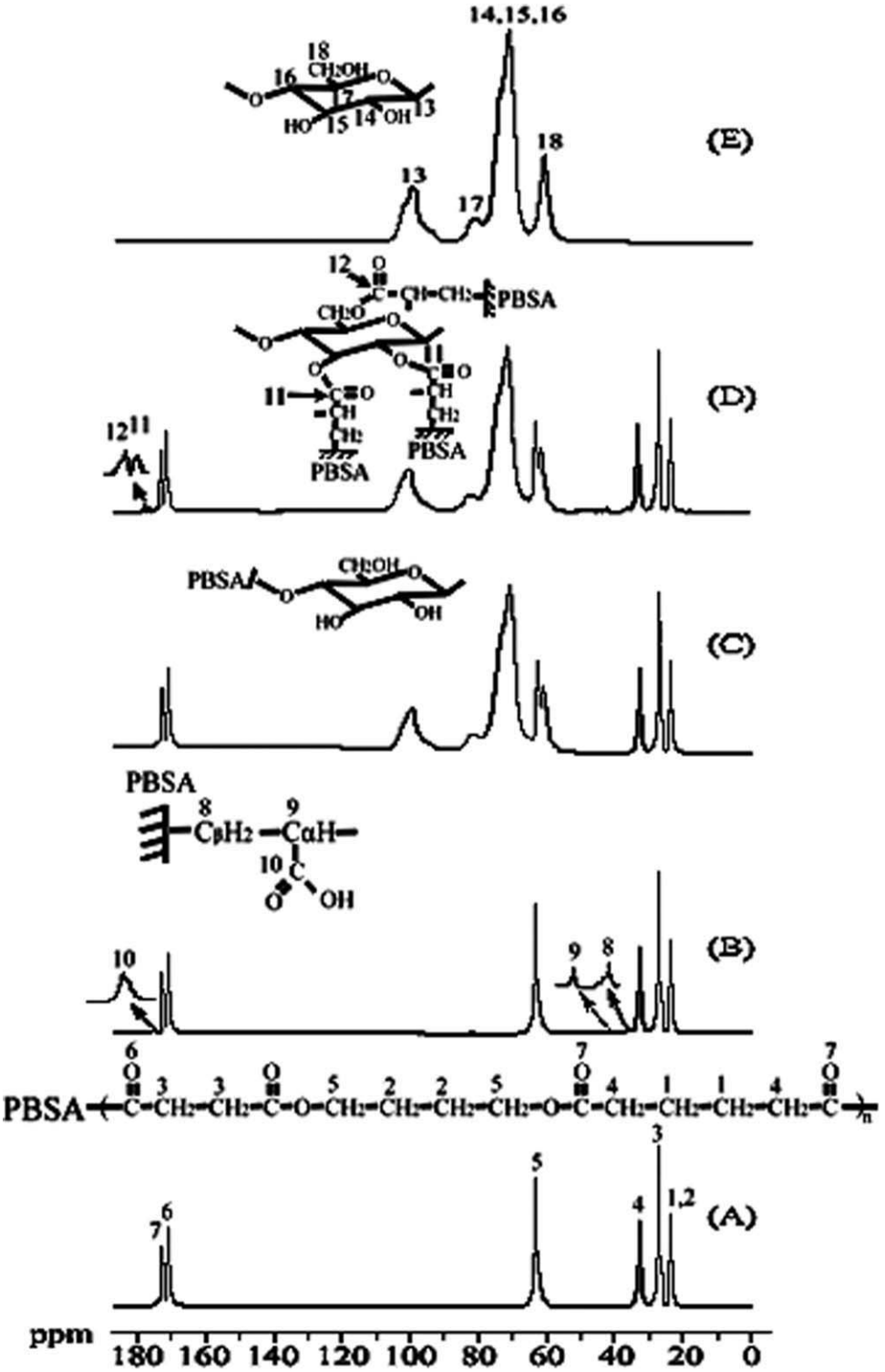

Figure 2 Solid-state ^{13}C-NMR spectra are shown for (A) PBSA, (B) PBSA-*g*-AA, (C) PBSA/BF (10 wt %), (D) PBSA-*g*-AA/BF (10 wt %), and (E) BF.

replicate samples in each dish. Therefore, each result is based on 15 samples.

Intrinsic viscosity

A Schott capillary viscometer was used to measure the intrinsic viscosity of PBSA and PBSA-*g*-AA/BF dissolved at various concentrations (0.5 g/dL, 1.0 g/dL, 1.5 g/dL, and 0.2 g/dL) in a chloroform solvent. Solutions were then cleared through a 0.45-μm filter (Lida Manufacturing Corp., Kenosha, WI). Subsequently, the capillary viscometer was filled with 10-mL of sample and equilibrated in a water bath

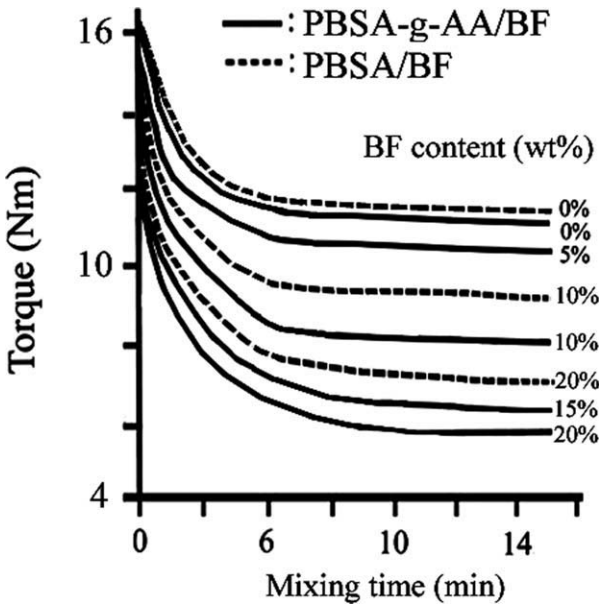

Figure 3 Torque values are plotted as a function of mixing time for PBSA/BF and PBSA-*g*-AA/BF blends with various BF content.

(Schott B801, Gruenplan, Germany) at 30°C ± 0.5°C. Each sample was passed through the capillary tube once before the flow time was measured. The flow time was used to calculate the relative viscosity and the reduced viscosity. The reduced viscosity was plotted as a function of PBSA or PBSA-*g*-AA/BF concentration with the *y*-intercept determining the intrinsic viscosity.

RESULTS AND DISCUSSION

Characterization of PBSA-*g*-AA/BF

FTIR spectra of unmodified PBSA and PBSA-*g*-AA are shown in Figure 1(A,B), respectively. The characteristic transitions of PBSA at 3300–3700, 1700–1760, and 500–1500 cm^{-1} appeared in the spectra of both polymers, with two extra shoulders observed at 1710 cm^{-1} in the PBSA-*g*-AA spectrum. These features are characteristic of acrylic acid carboxyl groups. Similar results have been reported previously.[23,24] The shoulders represent free acid in the modified polymer and, therefore, denote the grafting of AA onto PBSA. The FTIR spectrum of BF [Fig. 1(E)] exhibited peaks at 3241 cm^{-1} and 1063 cm^{-1} attributable to hydroxyl groups and —CO stretching, respectively.[25]

The peak assigned to the O—H stretching vibration at 3200–3700 cm^{-1} intensified in the PBSA/BF (10 wt %) composite [Fig. 1(C)] due to contributions from the —OH group of BF. The FTIR spectrum of the PBSA-*g*-AA/BF (10 wt %) composite in Figure 1(D) revealed a peak at 1737 cm^{-1} that was not present in the FTIR spectrum of the PBSA/BF (10 wt %) composite. This peak was assigned to the ester carbonyl stretching vibration of the copolymer. Bessadok et al.[26] also reported an absorption peak at 1740 cm^{-1} for this ester carbonyl group. These data suggest the formation of branched and crosslinked macromolecules in the PBSA-*g*-AA/BF by a covalent reaction of the carboxyl groups in PBSA-*g*-AA with the hydroxyl groups of BF.

To further confirm this finding, solid-state ^{13}C-NMR spectra of PBSA and PBSA-*g*-AA are compared in Figure 2(A,B), respectively. Three peaks were observed corresponding to carbon atoms in the unmodified PBSA (1,2: $\delta = 24.6$ ppm; 3: $\delta = 28.7$ ppm; 4: $\delta = 33.6$ ppm; 5: $\delta = 63.2$ ppm; 6: $\delta = 171.2$ ppm; 7: $\delta = 172.8$ ppm).[18] The ^{13}C-NMR spectrum of PBSA-*g*-AA showed additional peaks (8: $\delta = 42.1$ ppm; 9: $\delta = 36.1$ ppm; 10:—C=O $\delta = 175.2$ ppm), thereby confirming that AA was covalently grafted onto PBSA.

The solid-state ^{13}C-NMR spectra of PBSA/BF (10 wt %), PBSA-*g*-AA/BF (10 wt %), and BF are shown in Figure 2(C–E), respectively. Relative to unmodified PBSA/BF, additional peaks at $\delta = 42.1$ ppm (8) and $\delta = 36.1$ ppm (9) were observed in the spectra of composites containing PBSA-*g*-AA/BF. These same features were observed in previous studies[22] and indicate grafting of AA onto PBSA. However, the peak at $\delta = 175.2$ ppm (C=O) (10) [shown in Fig. 2(B)], which is also typical for AA grafted onto PBSA, was absent in the solid-state spectrum of PBSA-*g*-AA/BF (10 wt %). This was most likely the result of an additional condensation reaction between the carboxyl group of AA and the —OH group of BF that caused the peak at $\delta = 175.2$ ppm to split into two bands ($\delta = 177.1$ and 178.5 ppm). This additional reaction converted the fully acylated groups in the original BF to esters [represented by peaks 11 and 12 in Fig. 2(D)] and did not occur between PBSA and BF, as indicated by the absence of corresponding peaks in the FTIR spectrum of PBSA/BF (10 wt %) in Figure 2(C). The formation of ester groups significantly affects the thermal and biodegradation properties of PBSA-*g*-AA/BF, as discussed in greater detail in the following sections.

Torque measurements during mixing

The effects of BF content and mixing time on the melt torque of PBSA/BF and PBSA-*g*-AA/BF composites are shown in Figure 3. When preparing PBSA/BF or PBSA-*g*-AA/BF, the polymer was first melted, and the BF (fibrous state) was added to the melt. Torque values decreased with increasing BF content and mixing time, approaching a stable value when the mixture was sufficiently mixed after 8 min. To ensure complete mixing, blends were considered fully mixed after 15 min. The final torque values decreased with increasing BF content because the melt viscosity of BF was lower than that of either

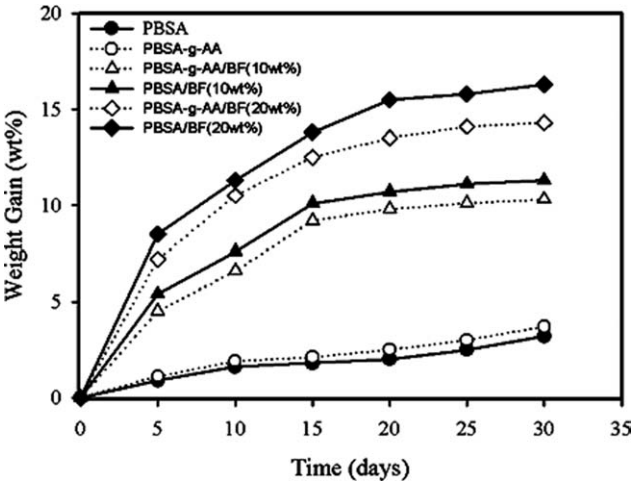

Figure 4 The percentage weight gain due to water absorption is shown for PBSA, PBSA-*g*-AA, PBSA/BF, and PBSA-*g*-AA/BF.

PBSA or PBSA-*g*-AA. Thus, for both blends, the melt viscosity of the entire composite was reduced through the addition of BF. In addition, the melt torque values of the PBSA-*g*-AA/BF composites were significantly lower than those of PBSA/BF composites at the same BF content. According to Kunanopparat et al.,[27] this improved rheological behavior is due to the formation of ester carbonyl groups (as discussed earlier), which induce conformational changes in the natural fiber molecule. Lei et al.[28] showed that the melt viscosity of an esterified natural fiber decreased with increasing reaction of the ester linkage between modified polymer and nutrient fiber.

Water absorption

At the same BF content, the PBSA-*g*-AA/BF composites exhibited a higher resistance to water absorption than did the PBSA/BF blend (Fig. 4). The water resistance of the PBSA-*g*-AA/BF composites was moderate, and it is proposed that the interaction of AA-grafted PBSA with BF increased the hydrophobicity of BF in this blend. For both PBSA/BF and PBSA-*g*-AA/BF, the percentage water gain over the 30-day test period increased with higher BF content. Because the polymer chain arrangement in these systems is supposedly random, the above result was likely due to decreased chain mobility with greater amounts of BF and to the hydrophilic character of BF, which adheres weakly to the more hydrophobic PBSA.

Biodegradation

Figure 5 shows that without the presence of nutrients, *A. baumannii* is a rod-shaped bacterium with approximate dimensions of 1.1–2.5 μm × 0.6–1.3 μm. Figure 5 also shows significant degradation of a PBSA/BF (10 wt %) matrix after encapsulation of *A. baumannii* for 10 days. This result suggested that the bacteria remained viable after having been entrapped in the polymer composites. Changes in the morphology of both PBSA and PBSA-*g*-AA/BF were noted as a function of the amount of time buried in an *A. baumannii* compost. SEM micrographs taken after 5, 10, and 20 days in the *A. baumannii* compost illustrate the extent of morphological change (Fig. 6). PBSA/BF (10 wt %) [Fig. 6(L–N)] exhibited larger and deeper pits, which appeared to be more randomly distributed, relative to those in the PBSA-*g*-AA/BF (10 wt %) composites [Fig. 6(F–I)]. These analyzes also indicate that biodegradation of the BF phase in PBSA/BF (10 wt %) increased with time, confirming the results presented in Figure 7.

After a 5-day incubation period, cell growth with gradual erosion and cracking was observed on the surface of the PBSA matrix [Fig. 6(B)]. After 10 days, the disruption of the PBSA matrix structure became more obvious [Fig. 6(C)]. This degradation was confirmed by increasing weight loss of the PBSA matrix with incubation time (Fig. 7), which reached nearly 15% after only 10 days. The most likely cause of this weight loss was biodegradation by *A. baumannii*. Bacterial degradation of PBSA has been previously reported,[29,30] and some have described degradation mechanisms involving enzymes such as lysozyme.[31,32] The results shown here indicate that *A. baumannii* is very effective at degrading PBSA.

The SEM micrographs in Figure 6 indicate that the PBSA-*g*-AA/BF (10 wt %) composites were more easily degraded than was pure PBSA. After a 5-day incubation period, the PBSA-*g*-AA/BF composite was coated with a biofilm of bacterial cells [Fig. 6(F)], indicating more cell growth than on PBSA at the same incubation time. Moreover, at 10 and 20

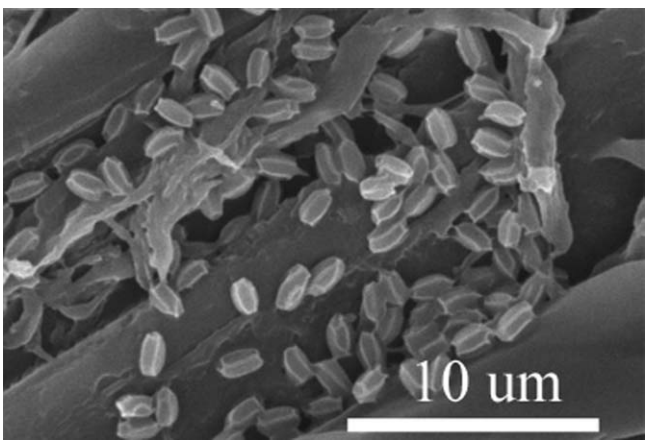

Figure 5 SEM micrographs show the morphology of PBSA-*g*-AA/BF (10 wt %, 10 days of compost incubation) composites loaded with *Acinetobacterbaumannii* (×5k).

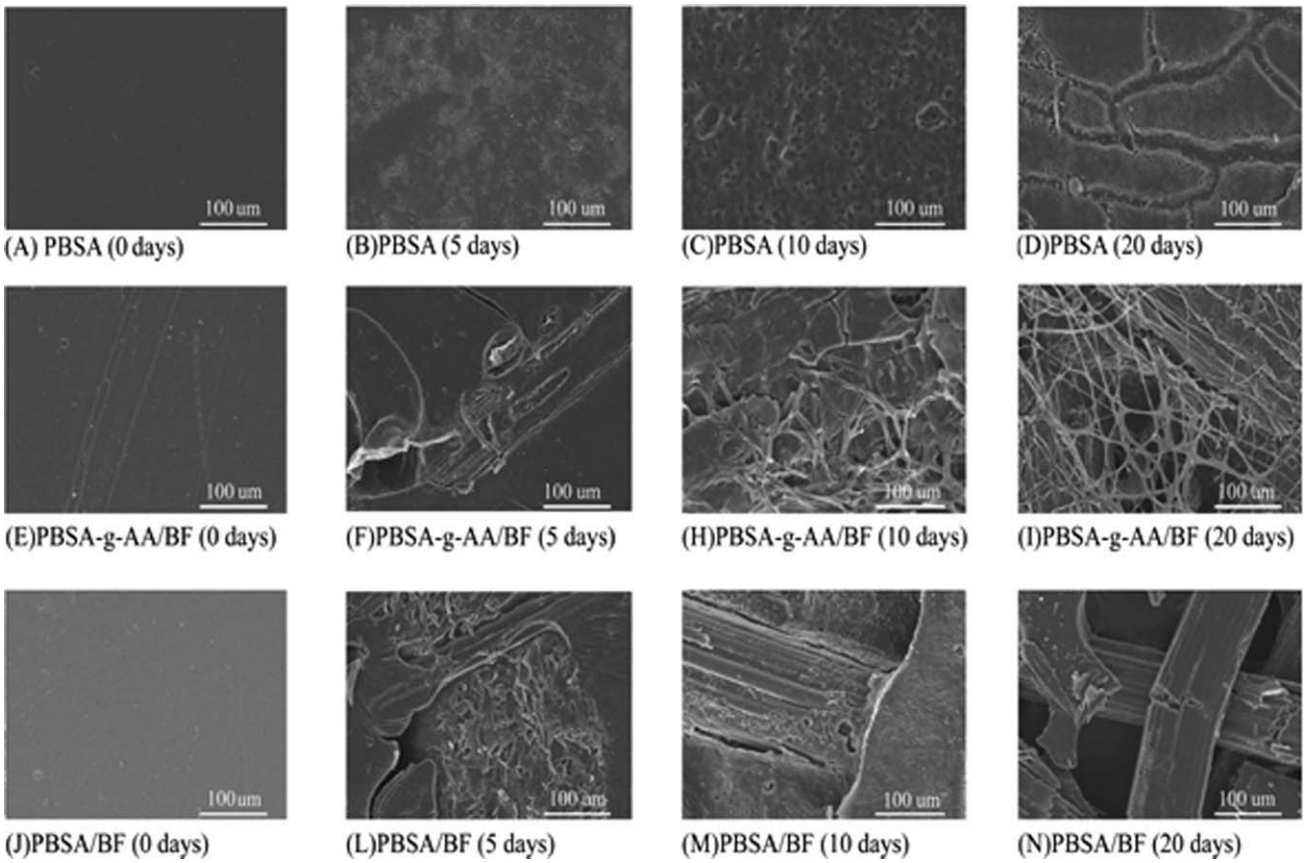

Figure 6 SEM micrographs show the morphology of PBSA (A–D), PBSA-*g*-AA/BF (E–I), and PBSA/BF (J–N) films as a function of incubation time in an *Acinetobacterbaumannii* compost.

days, larger pores were apparent on the PBSA-*g*-AA/BF composite [Fig. 6(H,I)], indicating a higher level of degradation. The degree of weight loss of the PBSA-*g*-AA/BF composites was also accelerated relative to that of PBSA, exceeding 75% after 30 days

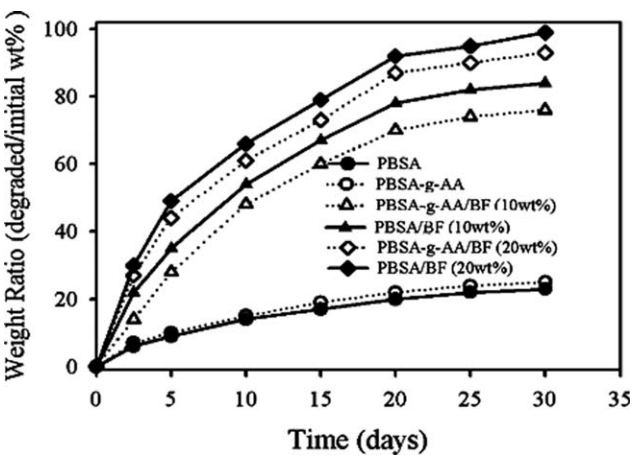

Figure 7 Weight loss percentages of PBSA, PBSA-*g*-AA, PBSA/BF, and PBSA-*g*-AA/BF are shown as a function of incubation time in an *Acinetobacter baumannii* compost.

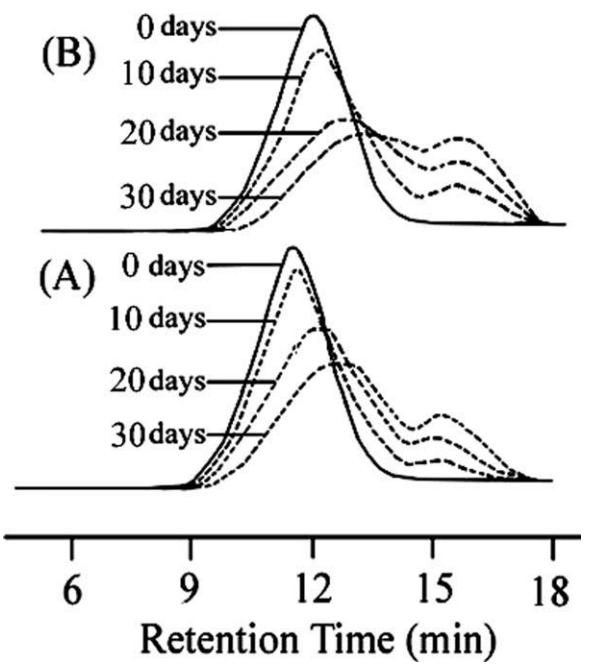

Figure 8 GPC retention times are given for (A) PBSA and (B) PBSA-*g*-AA/BF loaded with *Acinetobacter baumannii* cells.

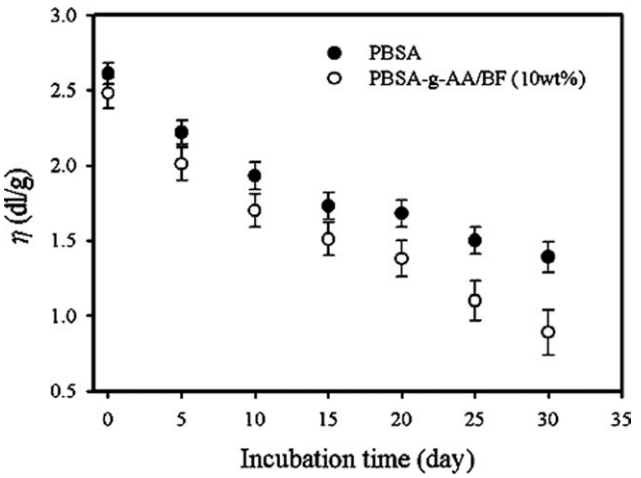

Figure 9 The intrinsic viscosity is plotted as a function of incubation time for PBSA and PBSA-*g*-AA/BF loaded with *Acinetobacter baumannii*.

(Fig. 7). These results clearly demonstrate that the addition of BF to the AA-grafted PBSA enhanced the biodegradability of the composite.

Figure 7 shows the percentage weight change, calculated using eq. (1), as a function of time for PBSA/BF and PBSA-*g*-AA/BF composites buried in the *A. baumannii* compost. In this environment, water diffused into the polymer causing swelling and enhanced biodegradation. As expected, the weight loss of PBSA is somewhat smaller than that PBSA-*g*-AA because the latter has better water absorption. For both the PBSA/BF and PBSA-*g*-AA/BF composites, the degree of weight loss increased with BF content. Composites with 20% BF degraded rapidly over the first 20 days, losing a mass equivalent to their approximate BF content, and showed a gradual decrease in weight over the next 10 days. PBSA-*g*-AA/BF exhibited a weight loss of $\sim$ 3 to 10 wt %.

Gel permeation chromatography and intrinsic viscosity

The biodegraded PBSA and PBSA-*g*-AA/BF composite samples were also analyzed using GPC. The results are presented in Figure 8(A,B). The retention times of major peaks (representing the original samples) increased with increasing incubation time because the macromolecules within the original samples were continuously broken down during the biodegradation process. Hence, the longer retention times observed for PBSA-*g*-AA/BF peaks also demonstrate its relatively higher biodegradability. In addition, a new peak appeared at $\sim$ 15–16 min after 10 days of incubation, suggesting that some molecular fragments were generated during biodegradation of the PBSA and PBSA-*g*-AA/BF composites. The formation of these fragments also implies that BF had been nearly depleted by this time. Zhao et al.[33] reported similar results. The retention time of these fragments was relatively consistent and may indicate that they were a product of bacterial utilization of the depolymerized matrix as a substrate, with consequent production of nearly uniform fragments.

The change in intrinsic viscosity and molecular weight as a function of incubation time for PBSA and the PBSA-*g*-AA/BF composite is shown in Figure 9. The intrinsic viscosity for PBSA with encapsulated *A. baumannii* ranged from 2.61 to 1.39 g/dL over the 30-day incubation period. The corresponding changes for PBSA-*g*-AA/BF were 2.48–0.89 g/dL. The lower intrinsic viscosity of the latter suggests a higher degree of polymer fragmentation. Additionally, the decreased intrinsic viscosity of PBSA-*g*-AA/BF may be due to conformational changes in the BF molecule caused by the previously discussed formation of ester groups. These results corroborate the findings of Seretoudi et al.,[34] which showed that the intrinsic viscosity of esterified PBSA fell with an increase in random hydrolysis of the ester group during biodegradation.

CONCLUSIONS

The compatibility and physical characteristics of BF with PBSA and acrylic acid-modified PBSA (PBSA-*g*-AA) were evaluated. FTIR and NMR analyses revealed the formation of ester groups in the resulting composites, formed by reactions between the hydroxyl groups in BF and the carboxyl groups of PBSA-*g*-AA. The PBSA-*g*-AA/BF composites were more easily processed due to lower mixing torques. Although the water resistance of PBSA-*g*-AA/BF was higher than that of PBSA/BF, the biodegradation rate when incubated with *A. baumannii* was only slightly lower. After 30 days, the PBSA-*g*-AA/BF (20 wt %) composite suffered a >93% weight loss. The degree of biodegradation increased with increasing BF content. Decreases in molecular weight and intrinsic viscosity were also greater for BF composites, suggesting a strong connection between biodegradability and these characteristics.

References

1. Unmar, G.; Mohee, R. Bioresour Technol 2008, 99, 6738.
2. Liu, L.; Yu, J.; Cheng, L.; Yang, X. Polym Degrad Stab 2009, 94, 90.
3. Wang, K. H.; Wu, T. M.; Shih, Y. F.; Huang, C. M. Polym Eng Sci 2008, 48, 1833.
4. Singh, S.; Mohanty, A. K.; Sugie, T.; Takai, Y.; Hamada, H. Compos A Appl Sci Manuf 2008, 39, 875.
5. Krzesińska, M. J.; Zachariasz, J.; Lachowski, A. I. Bioresour Technol 2009, 100, 1274.
6. Okubo, K.; Fujii, T.; Yamamoto, Y. Compos Part A Appl Sci Manuf 2004, 35, 377.

7. Kalia, S.; Kaith, B. S.; Kaur, I. Polym Eng Sci 2009, 49, 1253.
8. Bledzki, A. K.; Gassan, J. Prog Polym Sci 1999, 24, 221.
9. Okubo, K.; Fujii, T.; Thostenson, E. T. Compos Part A Appl Sci Manuf 2009, 40, 469.
10. Das, M.; Chakraborty, D. Ind Eng Chem Res 2006, 45, 6489.
11. Liu, H.; Wu, Q.; Han, G.; Yao, F.; Kojima, Y.; Suzuk, S. Compos Part A Appl Sci Manuf 2008, 39, 1891.
12. Mishra, S.; Naik, J. B.; Patil, Y. P. Compos Sci Technol 2000, 60, 1729.
13. Chin, X.; Guo, Q.; Mi, Y. J Appl Polym Sci 1998, 69, 1891.
14. Lee, S. H.; Wang, S. Compos Part A Appl Sci Manuf 2006, 37, 80.
15. Muller, R. J.; Kleeberg, I.; Deckwer, W. D. J Biotechnol 2001, 86, 87.
16. Kim, H. S.; Kim, H. J. Polym Degrad Stab 2008, 93, 1544.
17. Takasu, A.; Shibata, Y.; Narukawa, Y.; Hirabayashi, Y. Macromolecules 2007, 40, 151.
18. Ahn, B. D.; Kim, S. H.; Kim, Y. H.; Yang, J. S. J Appl Polym Sci 2002, 82, 2808.
19. Shah, A. A.; Hasan, F.; Hameed, A.; Ahmed, S. Biotechnol Adv 2008, 26, 246.
20. Ha, C. S.; Cho, W. J. Prog Polym Sci 2002, 27, 759.
21. El-Tayeb, N. S. M. Wear 2008, 265, 223.
22. Wu, C. S. J Controlled Release 2006, 132, 42.
23. Wu, C. S. Macromol Biosci 2005, 5, 352.
24. Zhao, H. P.; Zhu, J. T.; Fu, Z. Y.; Feng, X. Q.; Shao, Y.; Ma, R. T. Thin Solid Films 2009, 516, 5659.
25. Chang, S. T.; Yeh, T. F.; Wu, J. H. Polym Degrad Stab 2001, 74, 551.
26. Bessadok, A.; Roudesli, S.; Marais, S.; Follain, N.; Lebrun, L. Compos Part A Appl Sci Manuf 2009, 40, 184.
27. Kunanopparat, T.; Menut, P.; Morel, M. H.; Guilbert, S. Compos Part A Appl Sci Manuf 2008, 39, 777.
28. Lei, Y.; Wu, Q.; Yao, F.; Xu, Y. Compos Part A Appl Sci Manuf 2007, 38, 1664.
29. Uchida, H.; Nakajima-Kambe, T.; Shigeno-Akutsu, Y.; Nomura, N.; Tokiwa, Y.; Nakahara, T. FEMS Microbiol Lett 2000, 189, 25.
30. He, Y.; Asakawa, N.; Masuda, T.; Cao, A.; Yoshie, N.; Inoue, Y. Eur Polym J 2000, 36, 2221.
31. Ishii, N.; Inoue, Y.; Tagaya, T.; Mitomo, H.; Nagai, D.; Kasuya, K. I. Polym Degrad Stab 2008, 93, 883.
32. Ando, Y.; Yoshikawa, K.; Yoshikawa, T.; Nishioka, M.; Ishioka, R.; Yakabe, Y. Polym Degrad Stab 1998, 61, 1297.
33. Zhao, J. H.; Wang, X. Q.; Zeng, J.; Yang, G.; Shi, F. H.; Yan, Q. Polym Degrad Stab 2005, 90, 173.
34. Seretoudi, G.; Bikiaris, D.; Panayiotou, C. Polymer 2002, 43, 5405.